Synthesis, Crystal Structure, and Properties of Oxygen-Deficient Lanthanum Nickelate $LaNiO_{3-x}$ ($0 \leq x \leq 0.5$)

Toshihiro MORIGA,* Osamu USAKA, Tomomi IMAMURA, Ichiro NAKABAYASHI, Ichiro MATSUBARA,† Tsuneo KINOUCHI,†† Shinichi KIKKAWA,††† and Fumikazu KANAMARU†††

Department of Chemical Science and Technology, Faculty of Engineering, Tokushima University, Minami-Josanjima, Tokushima 770

† Government Industrial Research Institute of Osaka, Midorigaoka, Ikeda, Osaka 563

†† Faculty of Integrated Arts and Sciences, Tokushima University, Minami-Josanjima, Tokushima 770

††† The Institute of Scientific and Industrial Research, Osaka University, Mihogaoka, Ibaraki, Osaka 567

(Received August 5, 1993)

Two kinds of oxygen-deficient phases around $LaNiO_{2.5}$ were obtained by a low-temperature H_2 reduction of perovskite-type $LaNiO_3$. An antiferromagnetic $LaNiO_{2.5}$ with $T_N \cong 140$ K seems to be stoichiometric and a small amount of excess oxygen leads to a new ferromagnetic phases. A structural refinement has revealed that the former (space group $C2/c$) comprised one-dimensionally linked NiO_6 octahedra along the c-axis and NiO_4 square-planars connecting the octahedra chains. A cooperative Jahn–Teller distortion was observed in both coordination polyhedra, which suggested that $LaNiO_{2.5}$ has octahedral Ni^{3+} ions with the low-spin state and square-planar Ni^{+} ions. Its magnetic property and XPS spectrum support this model. The new ferromagnetism with $T_c \cong 230$ K could be understood due to a slight canting in the antiferromagnetic interaction between the octahedra and the square-planes.

Recently, copper oxides of the perovskite-type and related structures, such as La_2CuO_{4+x}, have been extensively studied with regards to superconductivity.[1,2] A non-copper oxide superconductor has not yet been found among transition metal oxides, except for $Li_{1+x}Ti_{2-x}O_4$.[3] Nickel oxides with a perovskite-related structure are antiferromagnetic, similar to copper oxides.

Metallic conductivity with Pauli-paramagnetism has been observed in trivalent nickelate $LaNiO_3$.[4] $LaNiO_3$ has a rhombohedrally-distorted perovskite-type structure isostructural with $LaCuO_3$. In the perovskite-type structure, the oxygen amount directly affects the magnetic and electrical properties. Control of the valence state of nickel ions without changing the basic structure would enable one to produce novel and interesting electrical and magnetic properties. Crespin et al. have reported that a low-temperature reduction of $LaNiO_3$ under H_2 gas has led to a new compound, $La_2Ni_2O_5$ (abbreviated $LaNiO_{2.5}$ hereafter), which could be indexed in the monoclinic system with the following parameters: $a=11.068$, $b=11.168$, $c=7.824$ Å, and $\beta=92.21°$.[5,6] They proposed the structural model of $LaNiO_{2.5}$ with Ni^{2+} located in both distorted octahedra and tetrahedra, i.e. a brownmillerite-type structure, determined by powder X-ray diffraction data and EXAFS spectroscopy. They also reported the presence of $LaNiO_2$ with monovalent Ni^{+}. $LaNiO_2$ is considered to be isostructural with an infinite-layer superconductor $(Ca,Sr)CuO_2$[7] or $(Sr,La)CuO_2$.[8] Rao et al. indexed the $LaNiO_{2.5}$ with a tetragonal cell of $a=7.816$ and $c=7.468$ Å and deduced that it had a new type of ordering with octahedral and square-planar coordinations of Ni^{2+}.[9,10] An electron diffraction study of the $LaNiO_{3-x}$ ($0 \leq x \leq 0.5$) system by Gonzalez-Calbet et al., showed the existence of a family of phases with the general formula $La_nNi_nO_{3n-1}$.[11] Although they basically agreed with Rao's structural model for $LaNiO_{2.5}$, their diffraction patterns could be indexed by Crespin's monoclinic unit cell better than Rao's. Additional crystal structural information is required. These authors gave little information about the electrical and magnetic properties of $LaNiO_{2.5}$ and its related phase with a chemical composition of around $LaNiO_{2.5}$. In this study, $LaNiO_{3-x}$ phases ($0 \leq x \leq 0.5$) were synthesized by a reduction of $LaNiO_3$ in H_2 flow at low temperatures. A Rietveld structural refinement of $LaNiO_{2.5}$ was carried out on powder X-ray diffraction data. The magnetic properties were measured and discussed in relation to the reduction process of $LaNiO_3$ to $LaNiO_{2.5}$.

Experimental

A polycrystalline sample of $LaNiO_3$ was prepared by a coprecipitation method. A solid-state reaction between La_2O_3 and NiO gave significant amounts of La_2NiO_4 and NiO as impurities. Then, the coprecipitation method was applied using aqueous solutions of $La(NO_3)_3 \cdot 6H_2O$ and $Ni(NO_3)_2 \cdot 6H_2O$ as starting materials. An aqueous solution of tetramethylammonium hydroxide (2.8 mol dm^{-3}) was added to form a sol of 1 : 1 metallic hydroxide. After washing with ethanol, the coprecipitant was dried at 200 °C in air and fired at 850 °C in an O_2 flow for 30 h to obtain the rhombohedral $LaNiO_3$.

$LaNiO_3$ was reduced in H_2 and N_2 gas mixtures with appropriate molar-ratios at various temperatures from 275 to 400 °C. The specimen used for the Rietveld analysis was obtained by annealing in diluted H_2 gas ($H_2 : N_2 = 1 : 99$, abbreviated as 1%-H_2/N_2 gas hereafter) at 350 °C for 16 h to improve its crystallinity. The gas flow rate was about 15 cm^3 min^{-1}. Powder X-ray diffraction data were collected using a Rigaku RAD-RB diffractometer with monochromatized Cu $K\alpha$ radiation (50 kV–150 mA). A step scanning technique was applied in measurements within the 2θ range from 20 to 100° for the Rietveld analysis. The stepping an-

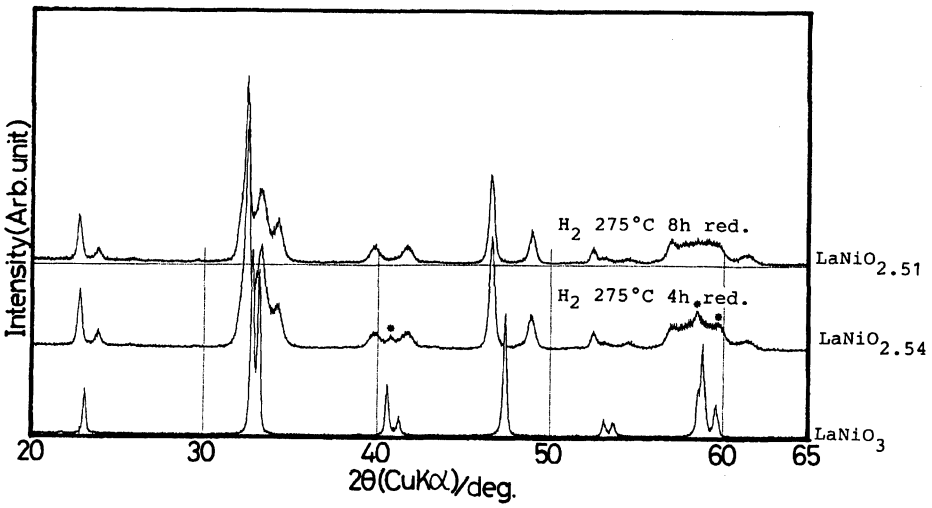

Fig. 1. Powder X-ray diffraction patterns of $LaNiO_{3-x}$ reduced under H_2 flow at 275 °C. The asterisks represent the peaks which could not be ascribed to either $LaNiO_3$ or $LaNiO_{2.5}$ reported by Crespin et al.[5]

gle was 0.02° and the measurement time was 10 s at each point. A simulation of the X-ray diffraction patterns and the Rietveld analysis were carried out by using the program "RIETAN" provided by Izumi.[12] The oxygen amounts of the samples were analysed using a Horiba EMGA-2800 device. The samples were reduced in a carbon crucible to convert their oxygen to carbon monoxide in He as a carrier gas. The amount of carbon monoxide was determined by measuring the IR absorbance.

The magnetic susceptibility was measured in the temperature range between 77 and 473 K by the Faraday method at a magnetic field strength of 0.9 T. Corrections were made in order to compensate for the diamagnetic susceptibility of the silica-glass bucket and the reduced specimens (e.g. $\chi_{dia} = -6.1 \times 10^{-5}$ emu mol^{-1} in $LaNiO_{2.5}$). XPS measurements were conducted for powdered samples pressed into a disk form immediately before the analysis. The instrument used was a Shimadzu ESCA-1000 device with Mg $K\alpha$ radiation (10 kV–30 mA). The resolution of the concentric hemispherical analyzer was higher than 0.1 eV. The binding energy (E_b) was calibrated with reference to the C1s level (284.8 eV). Ar-etching for the sample was carried out at a source power of 2 kV–20 mA.

Results and Discussion

Reduction Process of $LaNiO_3$ to $LaNiO_{2.5}$ and the Crystal Structure and Magnetic Property of $LaNiO_{2.5}$. Powder X-ray diffraction patterns of rhombohedrally-distorted perovskite-type $LaNiO_3$ and its reduced samples at 275 °C in H_2 flow for 4 and 8 h are shown in Fig. 1, respectively. The oxygen amounts z in $LaNiO_{2.5+z}$ of the reduced specimens were 0.04 and 0.01. All of the diffraction peaks of the product reduced for 8 h were consistent with those of $LaNiO_{2.5}$ reported by Crespin et al.[5] However, there were small peaks which could be ascribed to neither $LaNiO_3$ nor $LaNiO_{2.5}$ in the 4 h-reduced specimen. The magnetic properties were quite different between two kinds of the reduced specimens, as shown in Fig. 2. Although both specimens showed antiferromagnetic behavior below 140 K, an abrupt change in the susceptibility was found at about 230 K in the 4 h-reduced specimen. The phase giving the small diffraction peaks is responsible for this magnetism. The ferromagnetic phase is predominantly produced during an early step of the reduc-

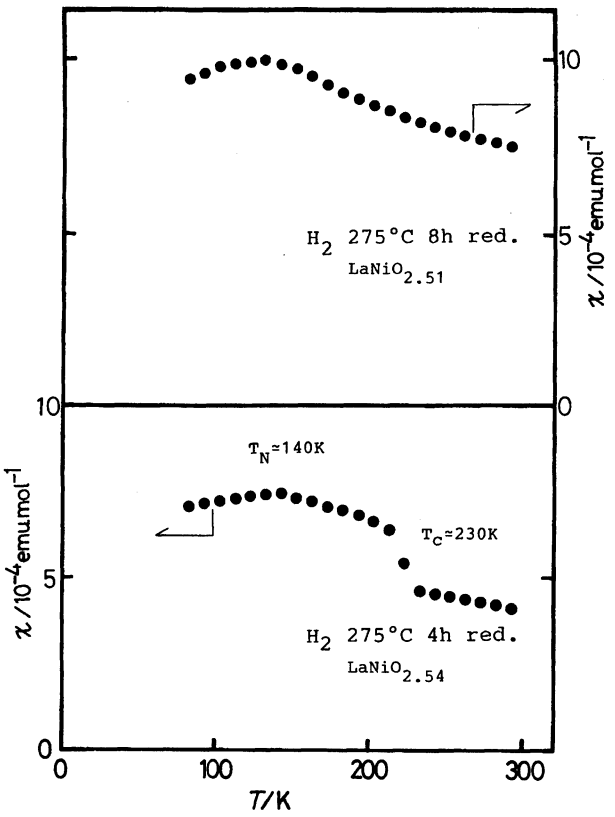

Fig. 2. Variations in the magnetic susceptibility in $LaNiO_{3-x}$ as a function of temperature.

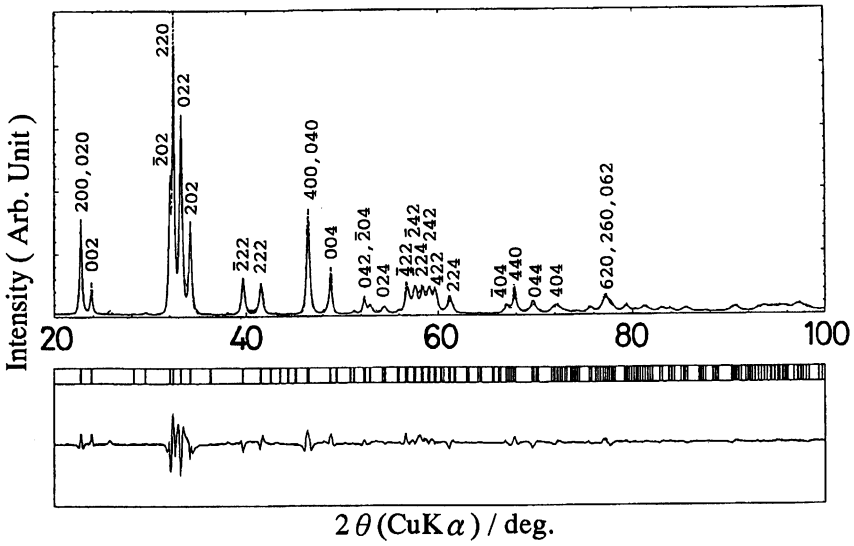

Fig. 3. Observed and calculated powder X-ray diffraction patterns, and their difference plots as a result of a Rietveld analysis of $LaNiO_{2.5}$.

tion. The ferromagnetic phase was also obtained in a reduction in a diluted H_2 flow, as described later. A further reduction led to La_2O_3 and an amorphous-like phase of nickel metal. Crespin et al. reported the presence of $LaNiO_2$ having a monovalent nickel ion which is isoelectronic to Cu^{2+}.[6] It was not obtained in the present experiment.

Since the as-reduced specimen under H_2 gas flow at 275 °C for 16 h had poor crystallinity, it was annealed under 1%-H_2/N_2 gas at 350 °C for 30 h. The oxygen amount of the product was $LaNiO_{2.48}$. We could index this product with a monoclinic cell of $a\cong7.83$, $b\cong7.80$, $c\cong7.47$ Å, and $\beta\cong93.7°$, related to the cubic perovskite by an expression of $2a_c\times2a_c\times2a_c$, although Rao et al. indexed the $LaNiO_{2.5}$ with a tetragonal cell having almost the same lattice lengths. A refinement of this structure proceeded by assuming a space group of $C2/c$[13] (unique axis b, cell choice 1) and the ideal composition of $LaNiO_{2.5}$. Initial coordinates were taken as follows: La, 8(f), (x,y,z), $x\cong y\cong z\cong0.25$; Ni(1), 4(a), (0, 0,0); Ni(2), 4(b), (0,1/2,0); O(1), 8(f), (x,y,z), $x\cong0.25$, $y\cong z\cong0$; O(2), 8(f), (x,y,z), $x\cong z\cong0$, $y\cong0.25$; O(3), 4-(e), $(0,y,1/4)$, $y\cong0$. The refinement was carried out in stage by stage; the atomic coordinates were fixed in initial calculations, but were subsequently allowed to vary after the scale, background, half-width and unit cell parameters so as to be close to their optimum values; finally, the thermal parameters were varied. When the isotropic thermal parameters were refined, those for the O(1), O(2), and O(3) sites had to be constrained to the same value. The preferred-orientations of the sample were not taken into account. The observed, calculated and difference plots of the result in the Rietveld analysis of $LaNiO_{2.48}$ are shown in Fig. 3. The final parameters for the refinement are summarized in Tables 1 and 2. The reliability factors exhibit rather high values, which may be due to the poor crystallinity for the Rietveld analysis. The integrated diffraction intensities agreed well between the observed and calculated values.

Figure 4 shows a schematic representation of the structure of $LaNiO_{2.5}$. This compound, $LaNiO_{2.5}$, comprises one-dimensionally linked NiO_6 octahedra along the c-axis and NiO_4 square-planars connecting the octahedra chains. The structure is basically the same as that of Rao's model.[9] However, the neighboring NiO_6 octahedra are slightly tilted and rotated in opposite directions. Its Ni K-edge XANES spectrum supports the presence of 4-fold square-planar Ni ions, not 5-fold pyramidal ones.[14] From another point of view, infinite $[NiO_{4/2}]$ layers can be considered to form the ab-plane.

The interatomic Ni(1)–O distances were 1.85 Å (to O (1) in the $[NiO_{4/2}]$ plane), 2.12 Å (to O(2) in the plane) and 1.87 Å (to O(3) perpendicular to the $[NiO_{4/2}]$ plane), respectively. The interatomic Ni(2)–O distances were 1.86 Å (to O(2)) and 2.13 Å (to O(1)). The distor-

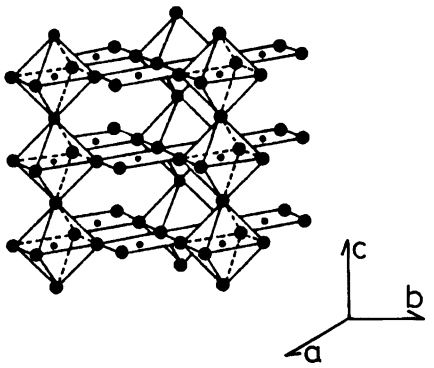

Fig. 4. Schematic representation of the structure of $LaNiO_{2.5}$. The large solid circles and small solid ones indicate oxide ions and Ni ions, respectively. Lanthanum ions are not shown for simplicity.

Table 1. Some Crystallographic Data Obtained by the Rietveld Refinement of $LaNiO_{2.48}$

Ideal composition	$LaNiO_{2.5}$		
Space group	$C2/c$		
Scale factor	0.00152(2)	Lattice constant a/Å	7.8329(8)
FWHM parameter U	1.8(3)	b/Å	7.7971(9)
V	−0.16(2)	c/Å	7.4739(7)
W	0.13(3)	β/°	93.693(6)
Asymmetry parameter	−0.13(1)	R_F/%[a]	2.65
Gaussian fraction	0.19(2)	R_p/%[b]	12.04
FWHM(Gauss)/		R_{wp}/%[c]	13.60
FWHM(Lorentz)	2.10(9)	R_e/%[d]	5.05
		R_I/%[e]	5.74

a) $R_F = \Sigma_k|[I_k(\mathrm{obs})]^{1/2} - [I_k(\mathrm{cal})]^{1/2}|/\Sigma_k[I_k(\mathrm{obs})]^{1/2}$, where $I_k(\mathrm{obs})$ and $I_k(\mathrm{cal})$ are the integrated observed and calculated intensities, respectively. b) $R_p = \Sigma_i|y_i(\mathrm{obs}) - y_i(\mathrm{cal})|/\Sigma_i y_i(\mathrm{obs})$, where $y_i(\mathrm{obs})$ and $y_i(\mathrm{cal})$ are the observed intensity and the calculated one, respectively. c) $R_{wp} = \{\Sigma_i w_i[y_i(\mathrm{obs}) - y_i(\mathrm{cal})]^2/\Sigma_i w_i y_i(\mathrm{obs})^2]\}^{1/2}$. d) R_e is the expected R_{wp}. e) $R_I = \Sigma_k|I_k(\mathrm{obs}) - I_k(\mathrm{cal})|/\Sigma_k I_k(\mathrm{obs})$.

Table 2. Positional and Isotropic Thermal Parameters of $LaNiO_{2.48}$

Atom	Position[a]	x	y	z	B/Å^2
La	8(f)	0.248(2)	0.241(2)	0.247(3)	0.43(17)
Ni(1)	4(a)	0	0	0	1.2(4)
Ni(2)	4(b)	0	1/2	0	1.0(2)
O(1)	8(f)	0.23(2)	0.06(1)	0.01(1)	2.3(14)[b]
O(2)	8(f)	−0.03(1)	0.27(1)	−0.01(1)	2.3[b]
O(3)	4(e)	0	0.01(2)	1/4	2.3[b]

a) Multiplicity and Wyckoff notation. b) Thermal parameters for oxygens were constrained to be equal each other.

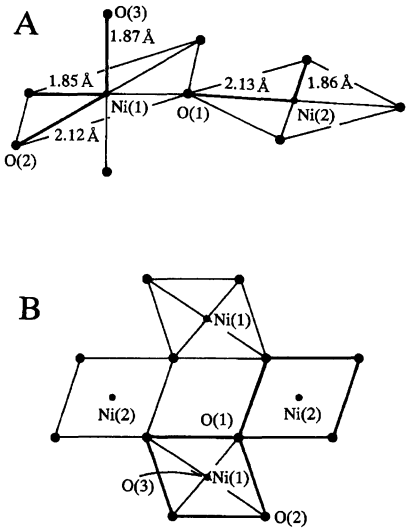

Fig. 5. A) Coordination polyhedra, $Ni(1)O_6$ and $Ni(2)O_4$, and the Ni–O distances in $LaNiO_{2.5}$. The solid circles represent oxide ions. B) Schematic view of the polyhedra from the c-axis. The area surrounded by the bold lines corresponds to the polyhedra shown in (A).

tion of the $[NiO_{6/2}]$ octahedra and the $[NiO_{4/2}]$ square-planar is appreciably large. A schematic drawing of the Ni–O coordination is shown in Fig. 5. An alternate arrangement of the longer and shorter Ni–O bond lengths in the $[NiO_{4/2}]$ plane was found. This manner is characteristic of a two-dimensional cooperative Jahn–Teller ordering, as seen in the perovskite-type $LaMnO_3$ with the d^4-Mn^{3+} ion.[15]

Two types of possible valency states of Ni ions in $LaNiO_{2.5}$ can be considered. One is that Ni^{2+} ions adopt a 6-fold octahedral and a 4-fold square-planar coordinations in the same proportion. Ni^{2+} ions have $3d^8$ electrons. The Ni^{2+} ion in an octahedral site is generally stable in the high-spin state with two unpaired electron in the e_g orbital. However, that in the center of a square-planar is stable in the low-spin state without any unpaired electrons. The cooperative Jahn–Teller ordering can arise only with high-spin d^4-, d^9- and low-spin d^7-transition-metal cations, which have one e_g electron.[16] In both coordination styles of the Ni^{2+} ions mentioned above, the cooperative Jahn–Teller ordering would hardly occur. The other is that the Ni^{3+} ion with $3d^7$ electrons adopts a 6-fold octahedral coordination and Ni^+ ion with $3d^9$ electrons adopts a 4-fold square-planar in analogy with Cu^{2+} ions. The low-spin d^7-Ni^{3+} and d^9-Ni^+ ions are of the Jahn–Teller types. It might be better to consider that the Ni(1) ions adopt a trivalent state in the octahedral coordination and that the Ni(2) ions adopt a monovalent state in the square-planar coordination.

The observed average interatomic $Ni^{3+}(1)$–O distance in this octahedron is 1.946 Å. This value agrees well with that of 1.91 Å, which is the effective ionic radius sum between the 6-fold Ni^{3+} with a low-spin state and the 2-fold O^{2-}.[17] The observed $Ni^+(2)$–O distance in this square-planar is 1.995 Å on the average. A gain of one electron increases the Ni–O distance by ca. 0.1 Å.[6] The interatomic Ni^+–O distance can, therefore, be

expected to be 1.94 Å, as follows:

$$0.49 \text{ Å (square-planar } Ni^{2+}) + 0.1 \text{ Å (increment)}$$
$$+1.35 \text{ Å (2-fold } O^{2-}) = 1.94 \text{ Å}.$$

This agrees well with the observed value. The Ni^{2+}–O distance in an octahedron with a high-spin state is estimated to be 2.04 Å, while that in a square-planar is estimated to be 1.84 Å. These values cannot explain the observed bond distances obtained in the present investigation. Compounds containing Ni^{+} ions have been known only in $LaNiO_2$,[6] $(La_{1.6}Sr_{0.4})NiO_{3.5}$,[18] and $LaSrNiO_{3.1}$.[19] Crespin et al., who had first synthesized $LaNiO_{2.5}$,[5] paid little attention to the valency states of the Ni ions. A comparison of the interatomic distances clarifies the presence of two kinds of Ni ions. It is very interesting that two kinds of the Ni ions coexist, having a difference of 2 in valence electrons.

Figure 6 represents the XPS spectra of $LaNiO_{3-x}$ in a binding energy region of 848 to 866 eV. The $Ni2p_{3/2}$ photoline of the spectrum of $LaNiO_3$ appeared at 855.5 eV (in Fig. 6a), which is in a good agreement with that in a previous paper.[20] The photoline at 851.0 eV was assigned to $La3d_{3/2}$. The binding energy of $Ni2p_{3/2}$ in Ni_2O_3 has been reported to be 855.9 eV.[21] The Ni ions in $LaNiO_3$ take only the trivalent state. Therefore, the observed line at 855.5 eV is attributable to the Ni^{3+} ion in $LaNiO_3$. After 3 min of Ar-etching, a novel and slight line at 852.5 eV appeared (Fig. 6b). It may be due to a reduction of Ni ions. The doublet photolines in the $Ni2p_{3/2}$ region of $LaNiO_{2.5}$ were observed at binding energies of 855.6 and 852.5 eV (Fig. 6c). The line assigned to $La3d_{3/2}$ was not clearly observed. The former line has the same energy as the Ni^{3+} ion. The energy of the latter is lower than that of divalent Ni^{2+} (853.5—854.0 eV in NiO),[21] and is almost equal to that of Ni metal (852.5 eV).[21] However, neither diffraction peaks nor ferromagnetism at room temperature due to Ni metal were detected in this specimen. It is reasonable to consider that the latter photoline is attributable to the Ni^{+} ion. At least two kinds of valence states of

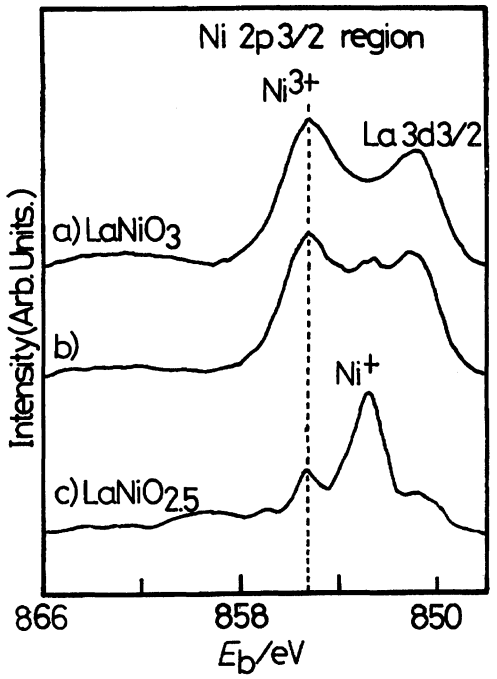

Fig. 6. Narrow scan XPS spectra in the $Ni2p_{3/2}$ region of a) $LaNiO_3$, b) Ar-etched $LaNiO_3$ for 3 min, and c) $LaNiO_{2.5}$.

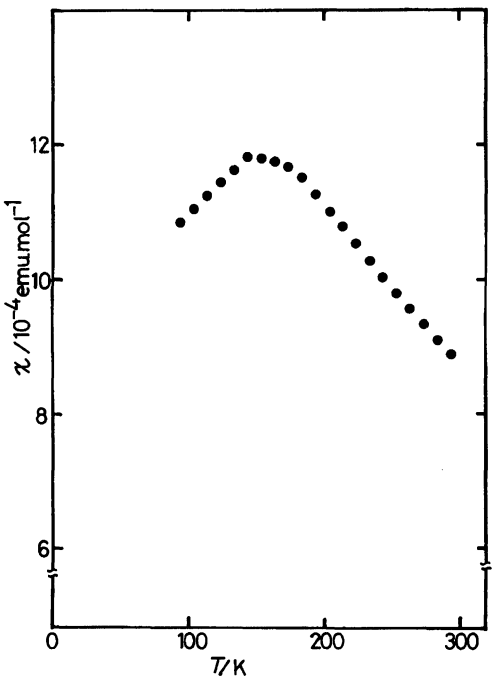

Fig. 7. Temperature dependence of the magnetic susceptibility of $LaNiO_{2.48}$.

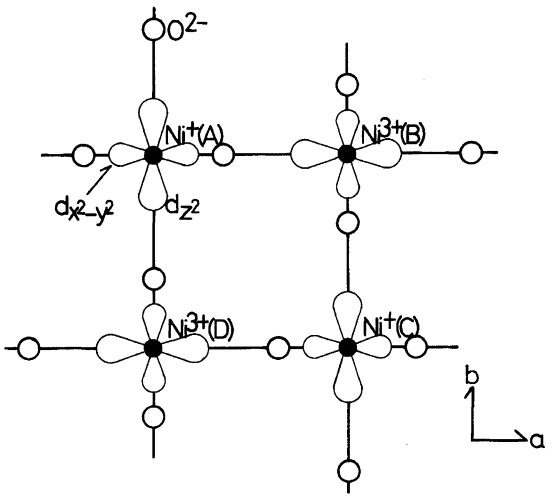

Fig. 8. Ordered arrangement of the $d_{x^2-y^2}$ and d_{z^2} orbitals in the $[NiO_{4/2}]$ plane in the structure of $LaNiO_{2.5}$. The elongated axis or orbital in the polyhedra is chosen as the z-axis or d_{z^2} orbital for convenience.

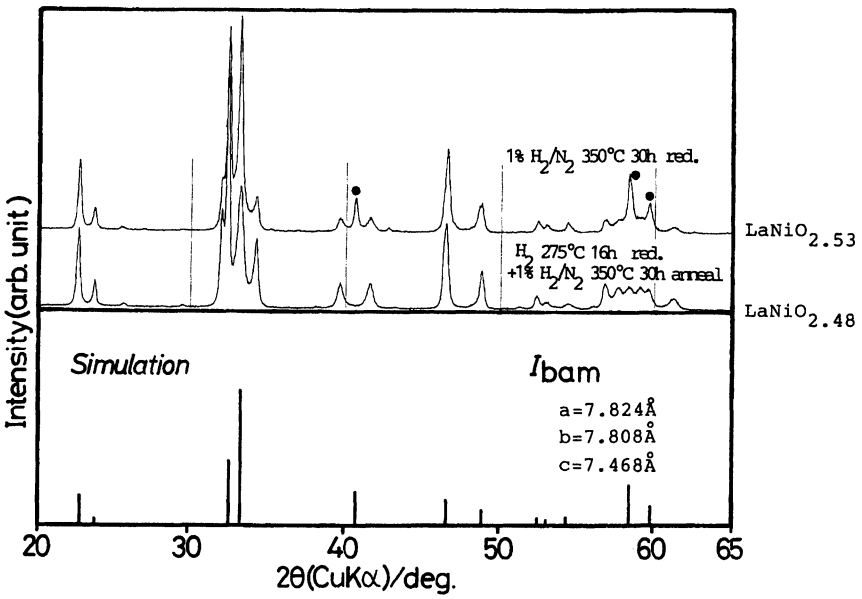

Fig. 9. Upper part; powder X-ray diffraction patterns of $LaNiO_{2.53}$ containing a ferromagnetic phase. Lower part; simulation of the diffraction pattern of the ferromagnetic phase. The peaks denoted as a solid circle are those characteristic of the orthorhombic ferromagnetic phase.

Ni ions coexist in $LaNiO_{2.5}$. One is Ni^{3+} and the other is lower than Ni^{2+}, which may be Ni^{+}.

Figure 7 represents the temperature dependence of the magnetic susceptibility of $LaNiO_{2.48}$. Its susceptibility almost obeyed a Curie–Weiss behavior above 140 K, and the effective magnetic moment was 1.8 μ_B per Ni ion. Since the Ni^{3+} ion in the low-spin state has one unpaired electron, the total spin angular momentum (S) is 1/2. That of the Ni^{+} ion with one unpaired electron is also 1/2. The effective magnetic moment calculated form the ideal $LaNiO_{2.5}$ with these spin configurations is 1.73 μ_B per Ni ion. This value is in a good agreement with the observed one.

The ordered arrangement of the $d_{x^2-y^2}$ and d_{z^2} orbitals in the $[NiO_{4/2}]$ plane in the structure of $LaNiO_{2.5}$ is shown in Fig. 8. Here, in case of discussing on the local arrangements of the orbitals of the Ni ions, the elongated axis in the NiO_6 octahedron or NiO_4 square-planar is defined as the z-axis for convenience. The cooperative Jahn–Teller effect makes the d_{z^2} orbital of the Ni^{+} ion directed to the $d_{x^2-y^2}$ one of the Ni^{3+} ion in the $[NiO_{4/2}]$ plane. In a similar matter, the d_{z^2} orbital of the Ni^{3+} ion directs to $d_{x^2-y^2}$ of the Ni^{+} ion. The strain energy of this type of ordering would be smaller than that resulting from a parallel orientation.

Intermediate Nonstoichiometric Phases $LaNiO_{2.5+z}$. By mildly reducing $LaNiO_3$ under 1%-H_2/N_2 gas at 350 °C for 30 h, we tried to obtain a well-crystallized single phase of this ferromagnetic specimen. Figure 9 shows the diffraction pattern of this reduced specimen. Its oxygen amount (z) was 0.03 in $LaNiO_{2.5+z}$. The ratio of this ferromagnetic phase to the antiferromagnetic $LaNiO_{2.5}$ increased compared to the previous specimen reduced under H_2 gas at 275 °C. The temperature dependence of the magnetization of $LaNiO_{2.53}$ is shown in Fig. 10, which also has a sharp drop at about 230 K.

A simulation of the diffraction pattern of the ferromagnetic phase is represented in the lower part of Fig. 9. The structural model used in this simulation was almost the same as the antiferromagnetic $LaNiO_{2.5}$, ex-

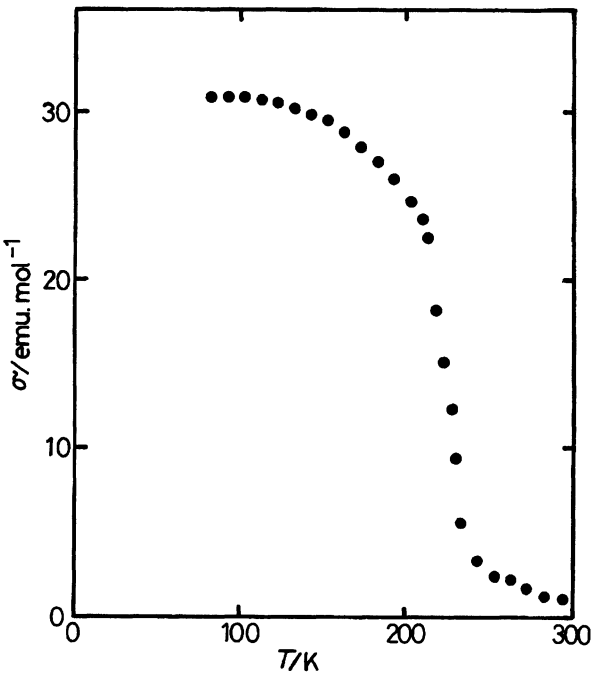

Fig. 10. Temperature dependence of the magnetization of $LaNiO_{2.53}$.

cept for using the space group of orthorhombic *Ibam* instead of that of monoclinic $C2/c$, which is equivalent to $I2/b$.[13] The space group of $C2/c$ is a maximal nonisomorphic subgroup of that of *Ibam*. Excess oxygen was assumed to occupy statistically the apical site between the two sheets of $[NiO_{4/2}]$ square-planar. The lattice constants were assumed to be a=7.824, b=7.808, and c=7.468 Å. This structural model can satisfactorily explain the diffraction pattern of $LaNiO_{2.53}$, especially the peaks denoted by a solid circle. The observed intensity of the peak appearing at about 41° is weaker than that appearing at about 47° in $LaNiO_{2.53}$. This is in conflict with the result of the simulation. It is due to the fact that this specimen is made up of ferromagnetic $LaNiO_{2.5+z}$ and antiferromagnetic $LaNiO_{2.5}$, and that the former peak is split into three peaks appearing around there. It is likely that the compound which had been reported by Rao et al.[9] to be orthorhombic $LaNiO_{2.5}$ comprises of this ferromagnetic phase. In the latest study, we could prepare the single ferromagnetic phase of $LaNiO_{2.60}$ by a vacuum reduction of $LaNiO_3$ with Al as an oxygen getter, which will be described in another paper.

Magnetic susceptibility measurements of La_2NiO_{4+y} have been reported in several papers.[22,23] A small cusp or break in the susceptibility near to 200 K was observed for nonstoichiometric $La_2NiO_{4.20}$. This anomaly has been interpreted in terms of the onset of an antiferromagnetic order with spins slightly canted out of the *ab*-plane. This phenomenon induced a net magnetic moment along the *c*-axis in the presence of an applied field. In $LaNiO_{2.5+z}$ with a slight nonstoichiometry, if its magnetic spin is supposed to lie in the same *ab*-plane as $La_2NiO_{4.20}$, this consideration would be applicable. In the infinite $[NiO_{4/2}]$ layers formed in the *ab*-plane, neighboring NiO_6 octahedra and NiO_4 square-planars were alternatively canted and rotated in opposite directions. The ferromagnetism appearing in $LaNiO_{2.5+z}$ ($z \cong 0.10$) may result from this spin canting out of the *ab*-plane.

We are grateful to Proferssor Kichiro Koto of Tokushima University, and Dr. Akira Yoshiasa of Hiroshima University, for useful information concerning the structural analysis. All computations were carried out at the Research Center for Protein Engineering, Osaka University.

References

1) J. D. Schirber, B. Morosin, R. M. Merrill, P. F. Hlava, E. L. Venturni, J. F. Kwap, P. J. Nigrey, R. J. Baughman, and D. S. Ginley, *Physica C (Amsterdam)*, **C152**, 121 (1988).
2) D. Jorgensen, B. Dabrowski, S. Pei, D. G. Hinks, L. Soderholm, B. Morosin, J. E. Shirber, E. L. Venturini, and D. S. Ginley, *Phys. Rev. B*, **38**, 11337 (1988).
3) D. C. Johnston, H. Prakash, W. Zachariasen, and R. Viswanathan, *Mater. Res. Bull.*, **8**, 777 (1973).
4) J. B. Goodenough and P. M. Raccah, *J. Appl. Phys.*, **36**, 1031 (1965).
5) M. Crespin, P. Levitz, and L. Gatineau, *J. Chem. Soc., Faraday Trans. 2*, **79**, 1181 (1983).
6) P. Levitz, M. Crespin, and L. Gatineau, *J. Chem. Soc., Faraday Trans. 2*, **79**, 1195 (1983).
7) T. Siegrist, S. M. Zahurak, D. W. Murphy, and R. S. Roth, *Nature*, **334**, 231 (1988).
8) G. Er, Y. Miyamoto, F. Kanamaru, and S. Kikkawa, *Physica C (Amsterdam)*, **C181**, 206 (1991).
9) K. Vidyasagar, A. Reller, J. Gopalakrishnan, and C. N. R. Rao, *J. Chem. Soc., Chem. Commun.*, **1985**, 7 (1985).
10) C. N. R. Rao, J. Gopalakrishnan, K. Vidyasagsr, A. K. Ganguli, A. Ramanan, and L. Ganapathi, *J. Mater. Res.*, **1**, 280 (1986).
11) J. M. Gonzalez-Calbet, M. J. Sayagues, and M. Vallet-Regi, *Solid State Ionics*, **32/33**, 721 (1989).
12) F. Izumi, *J. Miner. Soc. Jpn.*, **17**, 37 (1985).
13) "International Tables for X-Ray Crystallography," Kynoch Press, Birmingham (1974), Vol. IV.
14) T. Moriga, S. Kikkawa, M. Takahashi, F. Kanamaru, and I. Nakabayashi, *Jpn. J. Appl. Phys.*, **32**, Suppl. 32-2, 764 (1993).
15) J. B. Goodenough, "Magnetism and Chemical Bond," Interscience, New York (1963).
16) J. D. Lee, "A New Concise Inorganic Chemistry," 3rd ed, Van Nostrand Reinhold Co., Ltd., Berkshire (1977).
17) R. D. Shannon, *Acta Crystallogr., Sect. A*, **32**, 751 (1976).
18) M. Crespin, J. M. Bassat, P. Odier, P. Mouron, and J. Choisnet, *J. Solid State Chem.*, **84**, 165 (1990).
19) M. Crespin, C. Landron, P. Odier, J. M. Bassat, P. Mouron, and J. Choisnet, *J. Solid State Chem.*, **100**, 281 (1992).
20) J. L. G. Fierro and L. G. Tejuca, *Appl. Surf. Sci.*, **27**, 453 (1987).
21) D. Briggs and M. P. Seah, "Practical Surface Analysis by Auger and X-Ray Photoelectron Spectroscopy," John Wiley & Sons Ltd., Sussex (1983).
22) T. Freltoft, D. J. Buttrey, G. Aeppeli, D. Vaknin, and G. Shirane, *Phys. Rev. B*, **44**, 5046 (1991).
23) P. Gopalan, M. W. McElfresh, Z. Kakol, J. Spalek, and J. M. Honig, *Phys. Rev. B*, **45**, 249 (1992).